Real-Time Demonstration of Concurrent Upstream and Inter-ONU Communications in Hybrid OFDM DFMA PONs

Giddings, Roger; Tyagi, Tushar; Tang, Jianming

IEEE Photonics Technology Letters

DOI:
10.1109/LPT.2022.3227369

Published: 01/02/2023

Peer reviewed version

Real-time experimental demonstration of concurrent upstream and inter-ONU communications in hybrid OFDM DFMA PONs

Tushar Tyagi, *Member, IEEE*, R. P. Giddings, and J. M. Tang

***Abstract*—This paper presents the first real-time experimental demonstration of concurrent upstream and inter-ONU communications in a hybrid OFDM DFMA PON, enabled by a simple low-cost alteration to the remote node. Real-time FPGA-based DSP, incorporating a 128-pt FFT and a joint sideband processing technique, is used to demultiplex different sub-wavelength channels at the ONU and OLT receivers. The simple modification in the remote node removes the need for direct user-to-user data to pass via the OLT and core network thus providing ultra-low latency inter-ONU connectivity to support a variety of newly emerging latency sensitive 5G services. The presented PON is validated with two subwavelength bands, each capable of carrying one of two possible orthogonal channels (*I* or *Q*). The dynamic channel and subcarrier allocation allows flexible allocation of PON capacity between upstream and inter-ONU links for dynamic on-demand capacity allocation and also performance optimisation according to the different length dependent link characteristics. Moreover, the backscattering effect associated with upstream signals is shown to have negligible effect on the BER performance of the inter-ONU communications.**

***Index Terms*— Orthogonal frequency division multiplexing (OFDM), digital filter multiple access (DFMA), inter-ONU communication, passive optical networks (PON), hybrid OFDM DFMA PON**

I. INTRODUCTION

CENTRALIZED radio access network (C-RAN) architectures have gained great interest recently, as network providers view it as a key solution to decrease rollout difficulties and costs in small cell 5G networks. C-RANs also offer other advantages such as increased energy efficiency, low latency and a scalable and flexible network, which are key to fulfilling the requirements of 5G and beyond networks [1]. Mobile fronthauls (MFHs) form a critical segment of a C-RAN, connecting the centralized baseband units (BBUs) and radio units (RUs) typically employing the common public radio interface (CPRI) standard. However, current static MFHs are not spectrally and energy efficient when transmitting the digitized orthogonal frequency division multiplexing (OFDM) IQ waveform samples at fixed bitrates [2]. OFDM is employed for 5G signal modulation and is also expected to play a crucial role in future converged networks, as it offers a number of advantages such as high spectral efficiency, adaptive signal modulation according to channel characteristics, dynamic bandwidth allocation (DBA) with fine bandwidth granularity, trivial equalization through simple complex multiplication per subcarrier, as well as excellent tolerance to channel dispersion (CD) [3]. Furthermore, to achieve better bandwidth efficiency, channel aggregation is required to transmit a number of channels through a common transmission medium. To do this analog/digital signal processing (ASP/DSP) can be used [4], however, the DSP based techniques are more attractive due to their cost effectiveness. Furthermore, the DSP can be employed to realize flexible and reconfigurable transceiver architectures. To prove this, a digital filter multiple access passive optical network (DFMA-PON) is proposed in [5] employing shaping filters (SFs) in the transmitter to locate the different channels at their desired spectral locations. The DSP in the transmitter is designed to dynamically configure and allocate orthogonal channels (*I* and *Q*) to different subwavelengths (SW). This allows the transmission of different independent channels through the same medium. The matching filters (MF) at the receiver (one per channel) are used to extract the individual channels of interest. However, the DFMA technique can suffer performance degradation due to the non-flat physical channel response leading to cross-channel interference (CCI). To mitigate the effect of CCI in the DFMA PON, a cross-channel interference cancellation (CCIC) technique has been proposed and experimentally verified with real-time signal processing in [6] to show enhanced performance. The MF filter required per channel in addition to the DSP required for CCIC increases the computational burden on the technique as the number of channels increase. To address this, a hybrid OFDM DFMA PON has been introduced and numerically analyzed in [7] by employing a single FFT operation at the receiver to eliminate the MFs, thereby reducing the computational complexity. The aforementioned technique is experimentally verified with offline signal processing in [8] and shown to offer great relaxation in SF complexity requirement, reduction in the DSP complexity of the OLT receiver, drastic reduction in the maximum clock rate required at the OLT and enhanced performance as compared to the DFMA PON proposed in [5]. Moreover, the direct user-to-user services like virtual private

Manuscript received May 26, 2022; revised October 30, 2022; accepted December 2, 2022; Date of publication----------. This work was supported by the DSP Centre of Excellence funded by the European Regional Development Fund (ERDF) through the Welsh Government. (Corresponding author: *Roger Philip Giddings*.). The authors are with the School of Computer Science and Electronics engineering, Bangor University, Bangor, LL57 1UT, U.K.(e-mail:t.tyagi@bangor.ac.uk , r.p.giddings@bangor.ac.uk , j.tang@bangor.ac.uk)

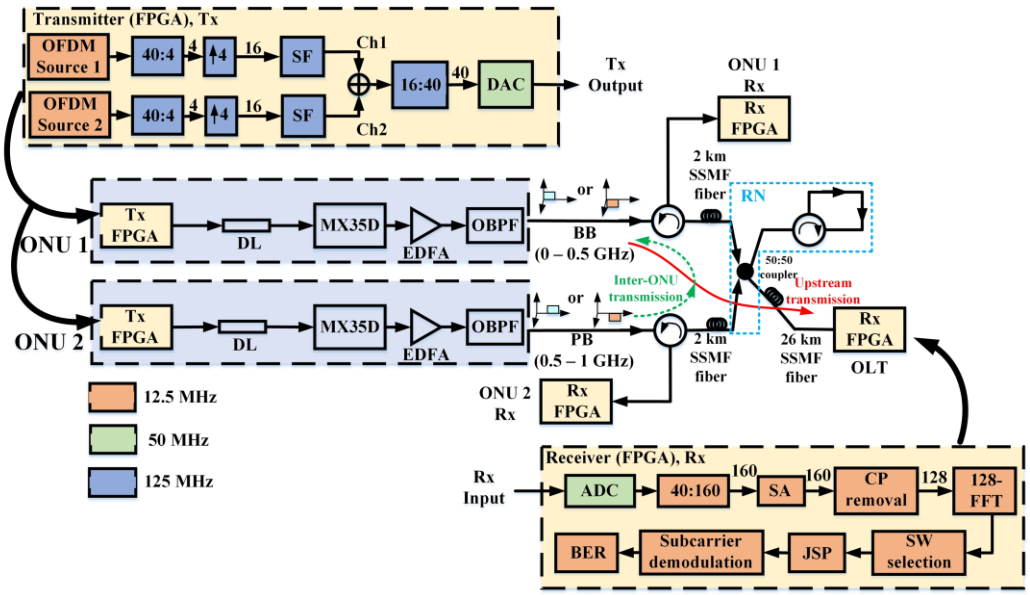

Fig. 1. Experimental set up for real time inter-ONU and upstream transmission and FPGA implemented DSP architectures. EDFA: Erbium doped fiber amplifier, OBPF: optical band pass filter, DL: delay line, RN: Remote node.

broadband connections, multimedia resource sharing and collaborative computing are latency sensitive where the fiber transmission induced latency plays a key role in determining the overall latency.

For the aforementioned PONs employing the conventional PON architecture, to provide inter-ONU data links, even if higher layer network functions can be bypassed, the traffic needs to be transmitted to the OLT, O-E-O converted, demodulated, and re-modulated at the OLT, and transmitted to the other ONU. This leads to a significant unwanted latency. Therefore, a highly desirable solution to reduce the end-to-end latency is to avoid the ONU-OLT-ONU transmission whilst only requiring a small modification to the PON architecture.

To this end, concurrent inter-ONU communication based on the hybrid OFDM DFMA PON is proposed and experimentally verified with offline signal processing in [9] by making simple alterations to the remote node (RN). This is performed by placing an optical circulator between one downstream output port and one upstream port of the RN coupler to redistribute and redirect the optical signal to each of the ONUs. The proposed network architecture is of course also applicable to fixed access network applications and not just the emerging low latency 5G applications. However, in order to technically verify the practical feasibility of the aforementioned technique, a real time experimental verification is critical. This paper presents a real time experimental validation of the aforementioned technique with FPGA-based real-time signal processing. Apart from the advantages described in [9], the demonstrated PON system offers the advantage of dynamic reconfigurability. This feature allows dynamic DSP-enabled RF spectral allocation of different channels to optimize performance. Furthermore, individual subcarriers (SC) within a single channel can be dynamically allocated to either upstream or inter-ONU communication as per the end-users' demands, as the upstream channels are effectively broadcast to the OLT and all ONUs. Moreover, since the bandwidth of the system here is 1 GHz, it is not affected by the optical backscattering effect.

II. Transceiver Architecture and Experimental Set Up

The experimental set up employed for the concurrent inter-ONU and upstream communication is shown in Fig.1. The set up consists of two independent ONUs, each with integrated FPGA based DSP to generate two independent OFDM channels: *I* (Cosine) and *Q* (Sine) signals, each located in either baseband (0 – 0.5 GHz) or passband (0.5 – 1 GHz). This results in 4 possible channels for transmission: *I* or *Q* in baseband and *I* or *Q* in passband. Each OFDM symbol consists of 40 parallel samples (32+8 cyclic prefix) which are converted to 4 parallel samples to optimize the resource usage. The 4 parallel samples are up-sampled by a factor of $M = 4$ to obtain 16 samples for generating the desired spectral images. The shaping filters (SF) employed are designed using the Hilbert transform approach described in [5] to locate the different channels at the desired spectral locations. The two OFDM signals are digitally added and produce 40 parallel samples at 50 MHz to fulfill the DAC interface requirements. Further details about the transmitter DSP architecture can be found in [6]. The DAC's electrical signal is fed to a MX35D linear transmitter from Thorlabs with an integrated tunable laser and Mach-Zehnder modulator (MZM) to generate an intensity modulated signal. To boost the optical output power from the MX35D, an Erbium doped fiber amplifier (EDFA) is used followed by an optical band-pass filter to filter out the out-of-band noise. The aforementioned equipment setup is identical for both ONUs, however an optical wavelength spacing (frequency spacing) of 0.4 nm (50 GHz) is adopted to avoid the optical beat interference (OBI) effect. The optical signals from both ONU1 and ONU2 each pass through optical circulators (for inter-ONU signal extraction) and 2 km of standard single mode fiber (SSMF) before being coupled via a 50:50 optical coupler at the RN. The combined optical output signal is transmitted to the OLT from the lower output port of the coupler for the 26 km upstream communication whereas an

TABLE I Key system parameters

Parameters	Values
IFFT/ FFT size	32/ 128
Subcarriers per channel	15
Up-sampling factor	4
Modulation format	16-QAM
Subcarrier spacing	15.625 MHz
DAC/ ADC sample rate	2 GS/s
Adopted FEC limit	1×10^{-3}
Optical launch power after OBPF	4.5 dBm
Ch1 & Ch2 optical wavelength	1550.1 & 1550.5 nm
PIN bandwidth	40 GHz
Amplitude at ADC input	≈ 400 mV

optical circulator is used at the upper port of the coupler to redirect the optical signal to each ONU for the inter-ONU communication. At the direct-detection (DD) receiver, a 40 GHz PIN (Thorlabs RXM40AF) converts the optical signal into an electrical signal. The amplitude of this electrical signal is optimized using the subsequent RF amplifier and attenuator stage. The optimized electrical signal is passed through a 1 GHz low pass filter (LPF) to filter out the out-of-band noise. The filtered signal is fed to the ADC and digitized at a sample rate of 2 GS/s for real-time signal processing. The same DSP is used for both the ONU and OLT receivers as shown in Fig.1. The received signal samples from the ADC are converted to 160 parallel samples, which corresponds to one symbol period, taking into account the original OFDM symbol length and the up-sampling factor of 4. A symbol alignment (SA) function is then applied to compensate for any symbol timing offset (STO) using dynamically programmable FPGA memory to manually optimize the STO value. The 32 cyclic prefix (CP) samples are then removed to obtain 128 samples corresponding to the FFT window. A 128-point FFT converts the 128 time domain samples in to 128 frequency bins, comprising of positive and negative frequencies. The 64 positive frequencies comprise of 32 lower frequency subcarriers (baseband) and 32 upper frequency subcarriers (passband). The SW selection block extracts either baseband or passband subcarriers. Further, due to the up-sampling induced double sideband (DSB) spectral images, each SW consists of 15 lower sideband (LSB) subcarriers (SC_L:1 – SC_L:15) and 15 upper sideband (USB) subcarriers (SC_U:15 – SC_U:1), which have conjugate symmetry (ignoring system induced impairments). The spectrum of the analogue signal at the ADC input at the OLT is shown in Fig.2 to understand the difference in performance of LSB and USB in the baseband and passband respectively. A similar ADC input signal spectrum is also observed at the ONUs. It can be observed that the LSB and USB undergo different gains in the baseband and passband due to the channel roll-off effect resulting in a 3 dB difference in SNR between LSB & USB in the baseband and passband respectively. To mitigate this effect, joint sideband processing (JSP) [10] is performed wherein the LSB and conjugated USB are added which results in a theoretical maximum increase in SNR of 3dB. The actual improvement can be <3 dB however due to channel roll-off and

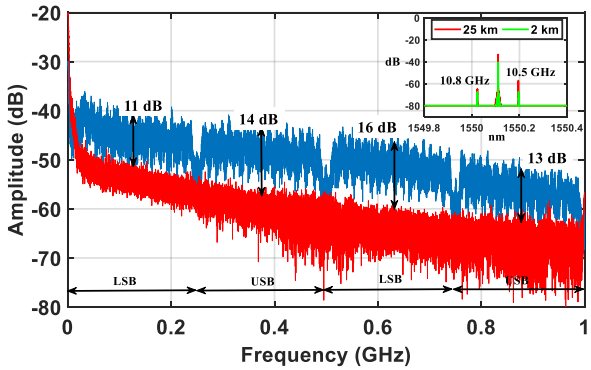

Fig. 2. Frequency spectrum of the input signal (signal+noise, blue) and noise (red) to the ADC with both SWs active.

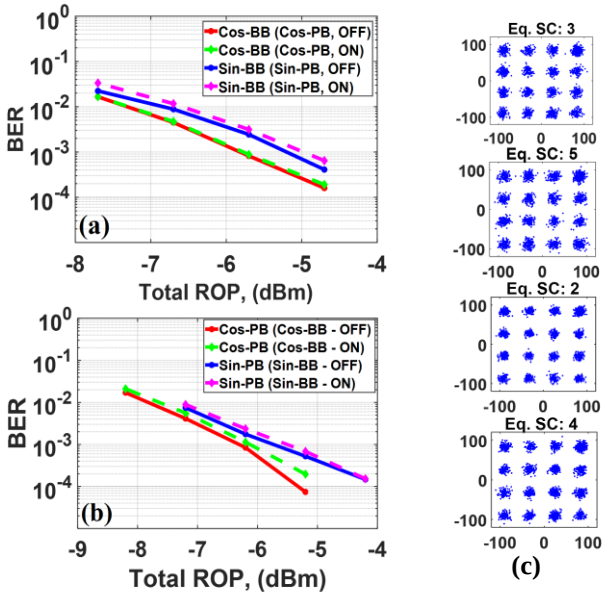

Fig. 3. Performance of *I* and *Q* channels, with the interfering SW on and off, for (a) BB (b) PB, (c) equalized example constellations for I-BB (SC:3 & 5), I-PB (SC:2 & 4).

the associated noise characteristics. The JSP block is designed to extract subcarriers from either LSB, USB or with JSP for further processing. Full details of the JSP technique can be found in [10]. The subcarriers within the output LSB/USB/JSP signal are demodulated before real-time error counting BER computation.

III. Experimental Results

The system performance is verified using the set up shown in Fig.1 with all adopted parameters listed in Table I. The performance for the upstream transmission, inter-ONU transmission and the penalty due to the RN are evaluated in terms of average BER vs. received optical power (ROP) for the 14 highest frequency SCs (SC:2 – SC:15). The BER is computed using the error count values extracted directly from the FPGA using the embedded logic analyzer tool. Performance is considered for the JSP case as it achieves the best performance [10]. The same procedure is applied to measure the performance of upstream and inter-ONU communication.

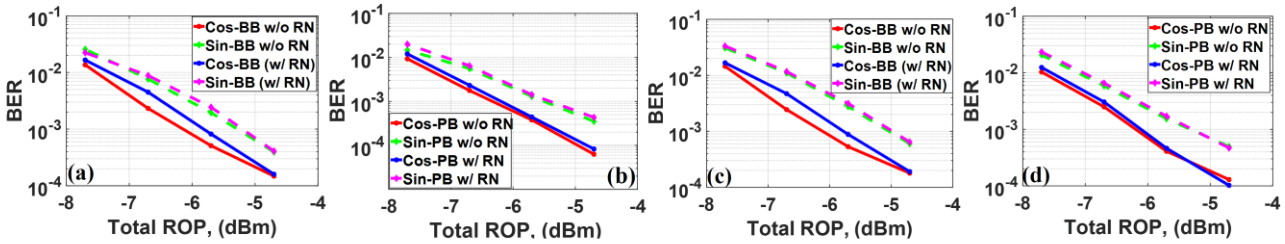

Fig. 4. Power penalty due to remote node modification for (a) BB only (b) PB only (c) BB (PB on) (d) PB (BB on).

A. Upstream performance

The BER performance for the upstream transmission is shown in Fig.3(a). The baseband (passband) SW is employed for upstream (inter-ONU) transmission for the case of either the *I* or *Q* channel. As shown in Fig.3(a), the ROP at the adopted FEC limit for the *I* (*Q*) baseband channel is -5.75 (-5.25) dBm respectively. Furthermore, the effect of interference from the inter-ONU channel is observed by switching the passband on and off via the DSP. The results show negligible interference effect as the two SWs occupy different spectral regions.

B. Inter-ONU performance

Here the passband SW is received at ONU 1, for the cases of either the *I* or *Q* channel transmitted from ONU 2. The procedure employed to measure BER performance is the same as in the upstream case and the results are shown in Fig.3(b). The ROP at the FEC limit for *I* (*Q*) channel is -6.25 (-5.75) dBm. The interfering channel in this case is the upstream channel in the baseband SW and Fig.3(b) shows the upstream channel has negligible effect on the performance of the inter-ONU communication. The results in Fig.3 thus validate the functional operation of the proposed PON architecture.

In the demonstrated PON the baseband (passband) is allocated to the upstream (inter-ONU) link. However, the SW channels can be received simultaneously at both the OLT and ONUs. Thus, the DSP enables the PON capacity to be flexibly allocated to either upstream or inter-ONU communications, at SW channel and subcarrier levels. This provides on-demand highly flexible, reconfigurability of the PON system capacity.

C. Upstream power penalty due to remote node modification

The power penalty for upstream transmission in the baseband (passband) channel due to the modification at the RN is evaluated by comparing the BER vs. ROP with and without the RN modification. For this purpose, the baseband (passband) channel is received at the OLT receiver with and without the RN modification, whilst maintaining all other conditions constant, also the passband (baseband) is switched off and on to observe any channel interference effects. The results are shown in Fig.4(a-d). As can be observed there is a worst-case power penalty at the FEC limit of <0.5 dB for the *I* channel in baseband (Fig.4(a)). Moreover, the effect of switching the interfering SW on and off for baseband (Fig.4(a) and (c)) and passband (Fig.4(b) and (d)) has negligible effect on the results.

Furthermore, the study of the penalty due to the remote node as shown in Fig.4(b) and 4(d) receives the passband at the OLT. This is equivalent to assigning the passband for upstream communication when the modified remote node is connected, and so the baseband could be allocated to inter-ONU communication. As clearly evident from Fig.4(b) and 4(d) similar performance is obtainable regardless of the baseband channel allocation. The small penalty due to the RN modification could be attributed to the Rayleigh backscattering-induced optical signal, since the associated fiber length is only 2 km, this explains the small penalty. To further study the backscattering effects in the inter-ONU transmission, the same experimental conditions as described in [9], are used. The optical spectrum at the ONU receiver is shown in the inset of Fig.2. The backscattering components namely Rayleigh (center), Brillouin anti-Stokes (left) and Brillouin Stokes (right) are separated by a frequency spacing of ≈ 10.8 GHz. However, the RF signal bandwidth employed in the current set up is only 1 GHz. Therefore, the Stokes and anti-Stokes components do not generate any undesired signal components, as shown in [9].

IV. Conclusion

A real-time hybrid OFDM DFMA PON, capable of supporting concurrent upstream and inter-ONU communications with a small RN alteration has been demonstrated. The system can dynamically allocate channels and subcarriers for upstream and inter-ONU links according to varying traffic conditions. A maximum upstream power penalty of <0.5 dBm is observed due to the RN modification. The reported work thus proves the technical feasibility of using the demonstrated technique in practical PONs to not only improve network flexibility and adaptability but also considerably reduce inter-ONU latency.

References

[1] A. Pizzinat *et al*., "Things you should know about fronthaul," *J. Light. Technol.*, vol. 33, no. 5, pp. 1077–1083, 2015.
[2] H. Zeng *et al*.,"Real-Time Demonstration of CPRI-Compatible Efficient Mobile Fronthaul Using FPGA," *J. Light. Technol.*, vol. 35, no. 6, pp. 1241–1247, 2017.
[3] R. Giddings, "Real-time digital signal processing for optical OFDM-based future optical access networks," *J. Light. Technol.*, vol. 32, no. 4, pp. 553–570, 2014.
[4] D. Wake *et al*.,"Radio over fiber link design for next generation wireless systems," *J. Light. Technol.*, vol. 28, no. 16, pp. 2456–2464, 2010.
[5] M. Bolea *et al.*, "Digital filter multiple access PONs with DSP-enabled software reconfigurability," *J. Opt. Commun. Netw.*, vol. 7, no. 4, pp. 215–222, 2015.
[6] E. Al-Rawachy *et al.*, "Experimental Demonstration of a Real-Time Digital Filter Multiple Access PON With Low Complexity DSP-Based Interference Cancellation," *J. Light. Technol.*, vol. 37, no. 17, pp. 4315–4329, 2019.
[7] Y. Dong *et al.*, "Hybrid OFDM-digital filter multiple access PONs," *J. Light. Technol.*, vol. 36, no. 23, pp. 5640–5649, 2018.
[8] W. Jin *et al.*, "Experimental Demonstrations of Hybrid OFDM-Digital Filter Multiple Access PONs," *IEEE Photonics Technol. Lett.*, vol. 32, no. 13, pp. 751–754, 2020.
[9] Z. Q. Zhong *et al.*, "Concurrent Inter-ONU Communications for Next Generation Mobile Fronthauls Based on IMDD Hybrid SSB OFDM-DFMA PONs," *J. Light. Technol.*, vol. 39, no. 23, pp. 7360-7369, 2021
[10] O. F. A. Gonem, *et al*., "Timing Jitter Analysis and Mitigation in Hybrid OFDM-DFMA PONs," *IEEE Photonics J.*, vol. 13, no. 6, pp. 1–13, 2021.